BIOCELL
2024 48(11): 1603-1612
ARTICLE

Tech Science Press

MPPa-PDT induced apoptosis and autophagy through JNK and p38 MAPK signaling pathways in A549 cells

Pinghua TU; Shanshan WANG; Kelan DENG; Xinjun LI; Zhanling WU*

Department of Respiratory and Critical Care Medicine, Xiaogan Hospital Affiliated to Wuhan University of Science and Technology, Department of Respiratory and Critical Care Medicine, Xiaogan, 432000, China

Key words: Photodynamic therapy, Lung carcinoma, Apoptosis, Autophagy

Abstract: Objectives: The antitumor effects of pyropheophorbide-α methyl ester-mediated photodynamic therapy (MPPa-PDT) were observed in several cancers. The objective of this investigation was to examine the antineoplastic efficacy of MPPa-PDT acting on lung carcinoma A549 cells and further elaborate mechanisms. **Methods:** The viability of A549 cells was examined with cell counting kit-8 after MPPa-PDT disposal. Hoechst 33342 staining, monodansylcadaverine (MDC) staining, and transmission electron microscopy were employed to observe apoptotic bodies and autophagic vesicles. Flow cytometry with Annexin V/propidium iodide (PI) labeling objectively assessed cell death. The expression of associated proteins, including Caspase-3, Beclin-1, LC-3II, and mitogen-activated protein kinase (MAPK) families concluding c-jun NH2-terminal kinase (JNK), p38 MAPK, and extracellular signal-regulated kinase 1/2 (ERK) were identified by Western blotting. **Results:** Prolonged exposure to MPPa-PDT gradually decreased lung cancer A549 cell viability. Apoptosis and autophagy activity were higher in the MPPa-PDT cohort in comparison to the control group. Meanwhile, autophagy inhibition enhanced cell-killing efficacy apparently. Besides, the JNK and p38 MAPK pathways were implicated in MPPa-PDT-triggered apoptosis and autophagy. **Conclusions:** This study demonstrated that JNK and p38 MAPK were engaged in MPPa-PDT-mediated apoptosis and autophagy in lung carcinoma A549 cells.

Introduction

Lung cancer has a high prevalence and fatality rate and poses a serious hazard to human health [1,2]. The diagnosis rate of lung cancer at an early stage is relatively poor due to insidious symptoms and ineffective screening methods. Therefore, many patients have been in the advanced stage when seeking medical advice. Conventional lung cancer treatment includes radiotherapy, chemotherapy, and surgery. In addition, targeted drug therapy and immunotherapy have improved survival prognosis significantly; however, the five-year overall survival outcome remains extremely low [3–5].

The emerging photodynamic therapy kills tumor cells directly and applies to treating various cancers [6,7]. It triggers a specific anti-tumor response and has the advantages of being less invasive, less toxic, more selective, and less resistant to drugs [8]. Numerous studies have shown that photodynamic therapy in combination with chemotherapy or immunotherapy can significantly enhance anti-tumor performance [9,10]. The photodynamic efficacy of novel photosensitizer methyl pyropheophenylchlorin has been widely explored in different carcinomas [11,12]. Some studies indicated that MPPa-PDT combined with cisplatin could effectively eliminate cancer cells with chemotherapy resistance by promoting apoptosis [13]. Recent research showed that MPPa-PDT induced autophagy to kill breast cancer cells via the protein kinase R-like endoplasmic reticulum kinase/eukaryotic initiation factor-2α (PERK/eIF2a) pathway [14]. In addition, our previous study manifested that MPPa-PDT induced lung cancer A549 cell death mainly through apoptosis pathways and cell cycle arrest [15]. Interestingly, MPPa-PDT treatment also triggered autophagy in A549 cells.

The crosstalk between autophagy and apoptosis in lung carcinoma is intricate. Autophagy, an evolutionarily conserved process, can be triggered in response to a variety of stresses to protect cells [16]. In addition, inhibition of autophagy can effectively kill cancer cells, making it a

*Address correspondence to: Zhanling Wu, 13477716060@163.com
Received: 26 May 2024; Accepted: 27 August 2024;
Published: 07 November 2024

Doi: 10.32604/biocell.2024.054364

potential cancer treatment [17]. Autophagy and apoptosis can be activated by the same stimulus. Wang et al. [18] implied that autophagy could protect gallbladder cancer cells from apoptosis, while inhibition of autophagy strengthened the antineoplastic effect both *in vitro* and *in vivo*. However, excessive activation of autophagy results in pro-apoptotic or autophagic programmed cell death [19]. In summary, a number of variables, such as cell species, photosensitizer trait, and photodynamic dose, may have an impact on the interplay between autophagy and apoptosis brought about by PDT. The relationship between autophagy and apoptosis in lung carcinoma is not yet clear.

In this research, we intended to explore MPPa-triggered apoptotic and autophagic responses in lung cancer A549 cells. We also tried to reveal the possible molecular mechanisms involved in the interplay between apoptosis and autophagy.

Materials and Methods

Resources

Roswell Park Memorial Institute (RPMI)-1640 cell culture medium (11875119), 10% fetal bovine serum (FBS, A5670701), and 1% penicillin-streptomycin mixture (10378016) were obtained from Gibco (Thermo Fisher Scientific, Waltham, MA, USA). Cell Counting Kit-8 was acquired from Beyotime (C0038, Shanghai, China). Sigma-Aldrich (St. Louis, MO, USA) provided Hoechst 33342 (14533), Pyropheophorbide-α methyl ester (MPPa, P3787), 3-methyladenine (3-MA, M9281), 2',7-Dichlorodihydrofluorescein-diacetate (DFCH-DA, D6883), Monodansylcadaverine (MDC, 30432), N-acetyl-L-cysteine (NAC, A7250), U0126 (662005), SB203580 (S8307) and SP600125 (S5567). BD Biosciences produced the Annexin V-FITC/PI apoptotic detection reagent (556547, Franklin Lake, NJ, USA). Antibodies for β-actin (4967S), Anti-rabbit IgG, HRP-linked Antibody (7074), Anti-mouse IgG, HRP-linked Antibody (7076), Caspase-3 (9664S), LC3A/B (4108S), Beclin-1 (3738S), p-JNK (4668S), JNK (9252S), p-p38 (4511S), p38 (8690S), p-ERK (4370S) and ERK (4695S) were sourced from Cell Signaling Technology (Danvers, MA, USA). Chongqing Jingyu Laser Technology Co. Ltd., offered PDT equipment apparatus (Chongqing, China).

Cell culture

Institute of Radiation Medicine, Peking Union Medical College (Beijing, China) supplied the lung carcinoma cell line A549 cells. The cells were authenticated using STR profiling and mycoplasma testing was used for examining contamination. No mycoplasma contamination and cross-contamination between cells were found. The cells were maintained in RPMI-1640 media, which contained 10% FBS and 1% penicillin-streptomycin, at 37°C in a humidified environment with 5% CO_2.

Cell treatment

The PDT equipment was utilized at a wavelength of 630 nm and an energy intensity of 40 mW/cm^2, as reported in the literature [15]. Cells were grouped by different processing modes as follows: Control group (no intervention), LED group (light irradiation, 630 nm, 40 mW/cm^2, 120 s), MPPa group (MPPa treatment for 20 h, then triple wash with phosphate-buffered saline (PBS) and replenish the medium), MPPa-PDT group (MPPa was first added and cultured for twenty hours; subsequently, substituted with fresh media after being washed three times with PBS, finally exposed to LED light irradiation). Some agents were preadded including NAC (5 mmol/L), 3-MA (5 mmol/L), SB203580 (10 μmol/L), SP600125 (20 μmol/L), or U0126 (20 μmol/L) before processing with MPPa-PDT. All of the above operations should be protected from light.

Cell viability analysis

CCK-8 was performed to evaluate cell viability based on the mechanism that WST-8 which was reduced by dehydrogenase activities in cells. Cell quantity was 5×10^3 per well and was cultivated in 100 μL of medium for 24 h. A549 cells were cultivated and 10 μL CCK-8 per well to incubated for 1 h. A microplate reader (Infinite 200 Pro, Tecan, Switzerland) was employed to measure the absorbance at 450 nm. Next, the proportion of cells in the experimental group compared to the control group was used to compute the cell viability. Based on the CCK-8 results, an MPPa concentration of 1 μmol/L and an intensity of PDT at 4.8 J/cm^2 were confirmed as experimental conditions in this study.

Determination of reactive oxygen species (ROS) accumulation

2',7-Dichlorodihydrofluorescein-diacetate (DCFH-DA) was applied to monitor intracellular reactive oxygen species levels. 5×10^4 cells/well were cultivated in 48-well plates for 24 h. A549 cells in each group were stained with (DCFH-DA) dye (10 μmol/L) for 10 min following different treatments. Then ROS generation was assessed by flow cytometry (Beckman Coulter CytoFLEX, Krefeld, Germany).

Hoechst and monodansylcadaverine (MDC) staining

Hoechst staining and MDC staining were employed for nuclei staining on apoptotic bodies and autophagy vacuoles labeling separately. A549 cells were then stained with Hoechst 33342 (10 μM) and MDC (0.05 mM) dye individually. Hoechst 33342 required staining for 5 min then assessed by 350 nm emission and 460 nm excitation wavelengths in fluorescence microscopy (Olympus BX-60, Tokyo, Japan). Similarly, MDC staining needed 10 min and was observed by fluorescence microscopy with 380 nm and 460 wavelengths for excitation and emission separately. Measurements of fluorescent intensity were conducted using Image-Pro Plus 7.0 software (Media Cybernetics, Rockville, MD, USA).

Transmission electron microscopy (TEM)

TEM was used to observe cellular ultrastructure. A549 cells were treated and then fixed at 4°C in a 2.5% glutaraldehyde solution, dehydrated using gradient ethanol, embedded, sliced, and stained for 30 min with uranyl acetate then for 15 min at 37°C using lead citrate for observation. At last, the specimens were observed under transmission electron microscopy (JEOL JEM-1400PLUS, Akishima-shi, Tokyo, Japan).

Flow cytometry for apoptosis evaluation

Annexin V-/PI staining was widely used for detecting apoptosis. To culture for 24 h, 5×10^3 cells were placed into the well of 96-well plates. The cells were divided into various groups (Control, MPPa, LED, 3-MA, MPPa-PDT, MPPa-PDT+3-MA) after appropriate disposal. At post-treatment 24 h, after harvesting the cells, they were centrifuged and treated for five minutes in darkness using Annexin V-FITC/PI apoptotic detection reagent (556547, NJ, USA), then measured by flow cytometry (Beckman Coulter CytoFLEX, Krefeld, Germany).

Western blot

To harvest the cell protein in different process groups. Protease and phosphatase inhibitors were added to RIPA buffer (P0013B, Beyotime, Shanghai, China) to lyse A549 cells. The protein concentration was subsequently determined using a BCA reagent (P0012, Beyotime, Shanghai, China). SDS-PAGE (PG111and PG113, EpiZyme, Shanghai, China) and following transferred onto polyvinylidene difluoride (PVDF) membranes (FFP32, Beyotime, Shanghai, China) resolved equal protein levels from each group. The membranes were treated using primary antibodies against β-actin (1:1500, anti-mouse, CST), Caspase-3 (1:1000, anti-rabbit, CST), LC3-II (1:1000, anti-rabbit, CST), Beclin-1 (1:1000, anti-rabbit, CST), p-JNK (1:1000, anti-rabbit, CST), JNK (1:1000, anti-mouse, CST), p-p38 (1:1000, anti-rabbit, CST), p38 (1:1000, anti-rabbit, CST), p-ERK (1:1000, anti-rabbit, CST) and ERK (1:1000, anti-rabbit, CST) and kept at 4°C overnight. Then the membranes were incubated with a secondary antibody (1: 2000, anti-rabbit IgG and anti-mouse IgG, CST) after rewarming and rinsing. The images were detected by ECL chemiluminescence system (Bio-Rad, Hercules, CA, USA) and then analyzed quantitatively by software.

Statistical analyses

The findings were examined using GraphPad Prism 6.0 (GraphPad Software LLC, Boston, MA, USA) and displayed as mean ± SD. A one- or two-way analysis of variance was employed to compare groups, while the SNK-q test was utilized to evaluate within groups. Each experiment was conducted a minimum of three times. Statistical significance was established at a threshold of $p < 0.05$.

Results

A549 cell activity was suppressed by MPPa-PDT

MPPa-PDT reduced A549 cell activity in a way that was dependent on both drug concentration and energy intensity, as Fig. 1A illustrates. In addition, neither the MPPa therapy nor the single LED treatment showed a discernible difference in cell viability ($p > 0.05$). In general, the viability of A549 cells decreased as the LED intensity and MPPa concentration increased, except 0.25 μmol/L MPPa combined with 1.2 J/cm^2 light dose, which did not exhibit any significant inhibition ($p < 0.05$). The experiment condition (1 μmol/L MPPa integrated with light intensity at 4.8 J/cm^2) was confirmed according to the half-maximal inhibitory concentration (IC50) values. Cell death was 48.5% ± 1.2% in response to processing with 1μmol/L MPPa and a PDT dosage of 4.8 J/cm^2. After MPPa-PDT treatment, the cell activity was evaluated by CCK-8 at 0, 3, 6, 12, and 24 h, respectively. The results demonstrated that MPPa-PDT inhibited A549 cell viability as time prolonged (Fig. 1B).

MPPa-PDT caused ROS accumulation in A549 cells

Treating tumors via ROS-based pathways has been recognized as a reasonable approach. Moreover, ROS production has a vital significance in cancer treatment by PDT. Therefore, ROS accumulation was evaluated by flow cytometry using a DCFH-DA probe. Our results revealed that MPPa-PDT induced ROS, while no ROS was detected in MPPa or LED groups (Fig. 2A,B). We then investigated whether ROS played a role in the development of autophagy and apoptosis. Our results revealed that pretreatment with ROS inhibitor NAC markedly decreased Caspase-3 and LC3-II expression (Fig. 2C,D), indicating that MPPa-PDT-triggered autophagy and apoptosis were induced by elevated levels of ROS. These findings were consistent with the previous

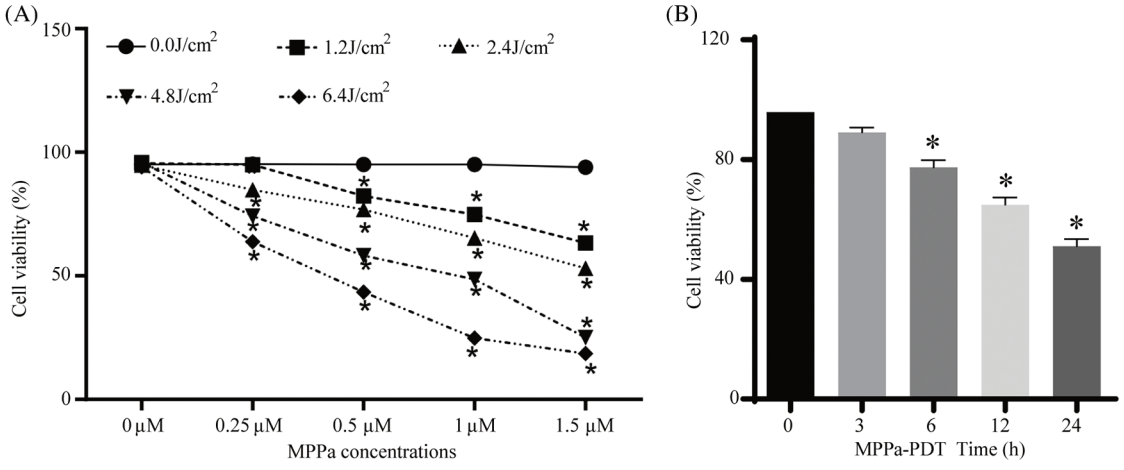

FIGURE 1. (A) MPPa-PDT lowered A549 cell viability. The cells were subjected to a variety of energy intensities (0, 1.2, 2.4, 4.8, 6.4 J/cm^2) in conjunction with varying drug doses (0, 0.25, 0.5, 0.75, 1.5 μmol/L). (B) Cell viability was assessed at various points (0, 3, 6, 12, 24 h) following MPPa-PDT processing. *$p < 0.05$ in comparison to the control group.

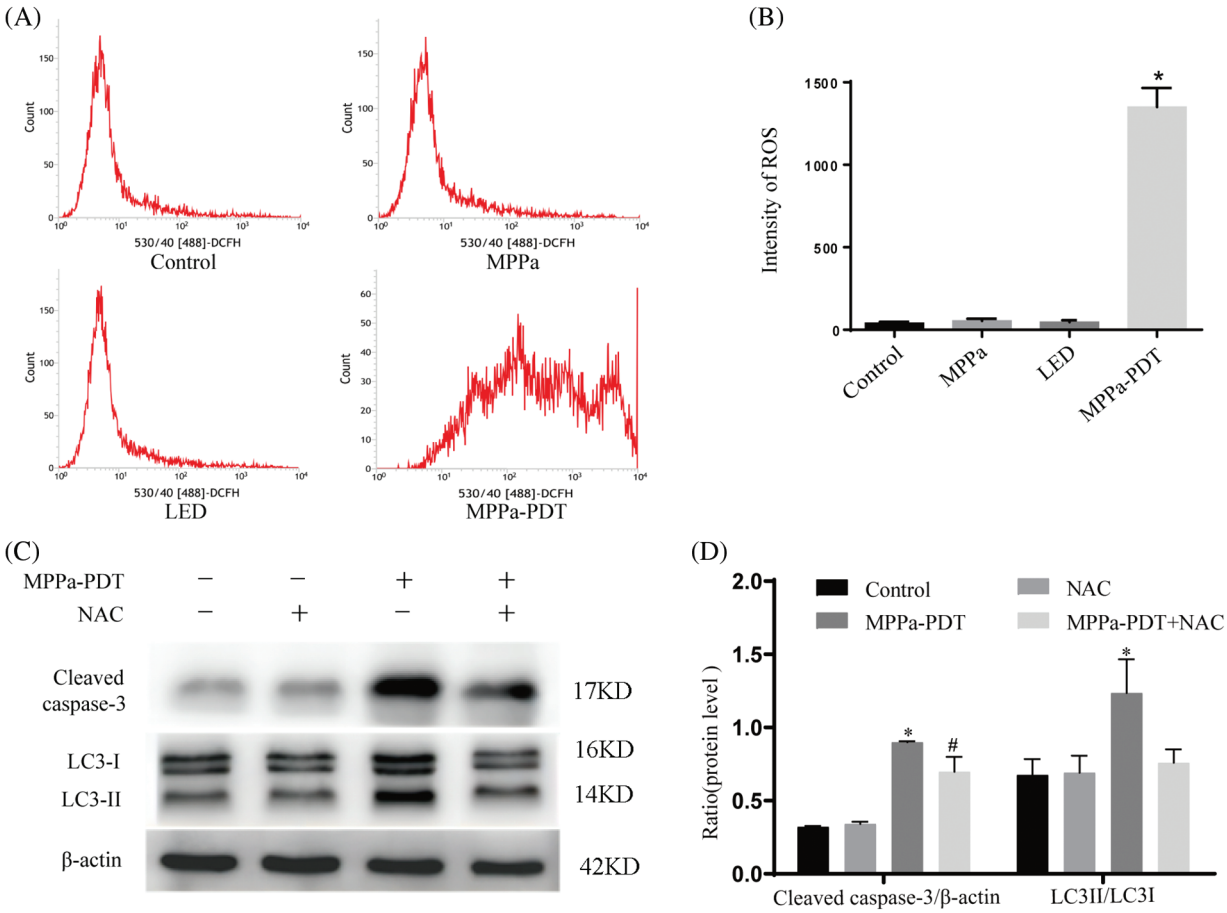

FIGURE 2. Accumulation of ROS following MPPa-PDT administration. (A, B) ROS level was determined by flow cytometry. *$p < 0.05$ compared to the control group. (C, D) MPPa-PDT upregulated the expression of Caspase-3 and LC3 II; however, pretreatment with NAC (ROS inhibitor, 5 mM) could decrease the expression. Three iterations of the experiments were conducted. *$p < 0.05$ *vs.* control group; #$p < 0.05$ compared with the MPPa-PDT group.

studies demonstrating that PDT-mediated apoptosis and autophagy process depend on the ROS level and photosensitizer type [20,21].

MPPa-PDT therapy resulted in apoptosis and autophagy of A549 cells

Hoechst staining, MDC staining, and Western blot were applied to verify the apoptosis and autophagy in this experiment. Typical apoptosis was identified as chromatin condensation, which could be detected by Hoechst staining (Fig. 3A). Autophagic vacuoles were characterized by the accumulation of green spots around the nucleus (Fig. 3B). Massive apoptotic cells and autophagic vacuoles appeared in MPPa-PDT group compared with other groups. In addition, autophagy and apoptosis marker proteins were detected by Western blot (Fig. 3C,D). Our results revealed that MPPa-PDT management significantly upregulated Caspase-3, Beclin-1, and LC3 II levels.

Features of ultrastructure changed after MPPa-PDT intervention

TEM was employed to observe the disappearance of pseudopodia structure and alterations in cell morphology following MPPa-PDT processing, as illustrated in Fig. 4. In the MPPa-PDT group, autophagosomes with double-membrane vacuoles containing degraded cellular organelles, meanwhile, apoptotic bodies with characteristics of nucleus degradation and condensation were observed (Fig. 4B,C). Nevertheless, the control group did not exhibit any apoptotic bodies or autophagosomes (Fig. 4A).

The link between apoptosis and autophagy attributable to MPPa-PDT

Further confirming if autophagy was involved in MPPa-PDT-induced cell death, 3-methyladenine (3-MA) was used which was a classical repressor of autophagy. Annexin V/PI staining was implemented to evaluate apoptosis via flow cytometry. Compared to the control group, the MPPa-PDT group displayed a greater death rate according to this study (Fig. 5A,B). Moreover, pretreatment with 3-MA united MPPa-PDT processing significantly boosted the cell apoptotic rate ($p < 0.05$). These findings showed that autophagy suppression enhanced death whereas MPPa-PDT caused A549 cells apoptosis. The results were consistent with previous studies demonstrating that autophagy played a protective role in cell death [22]. However, its protection mechanism still needs further research due to the complex relationship between autophagy and apoptosis.

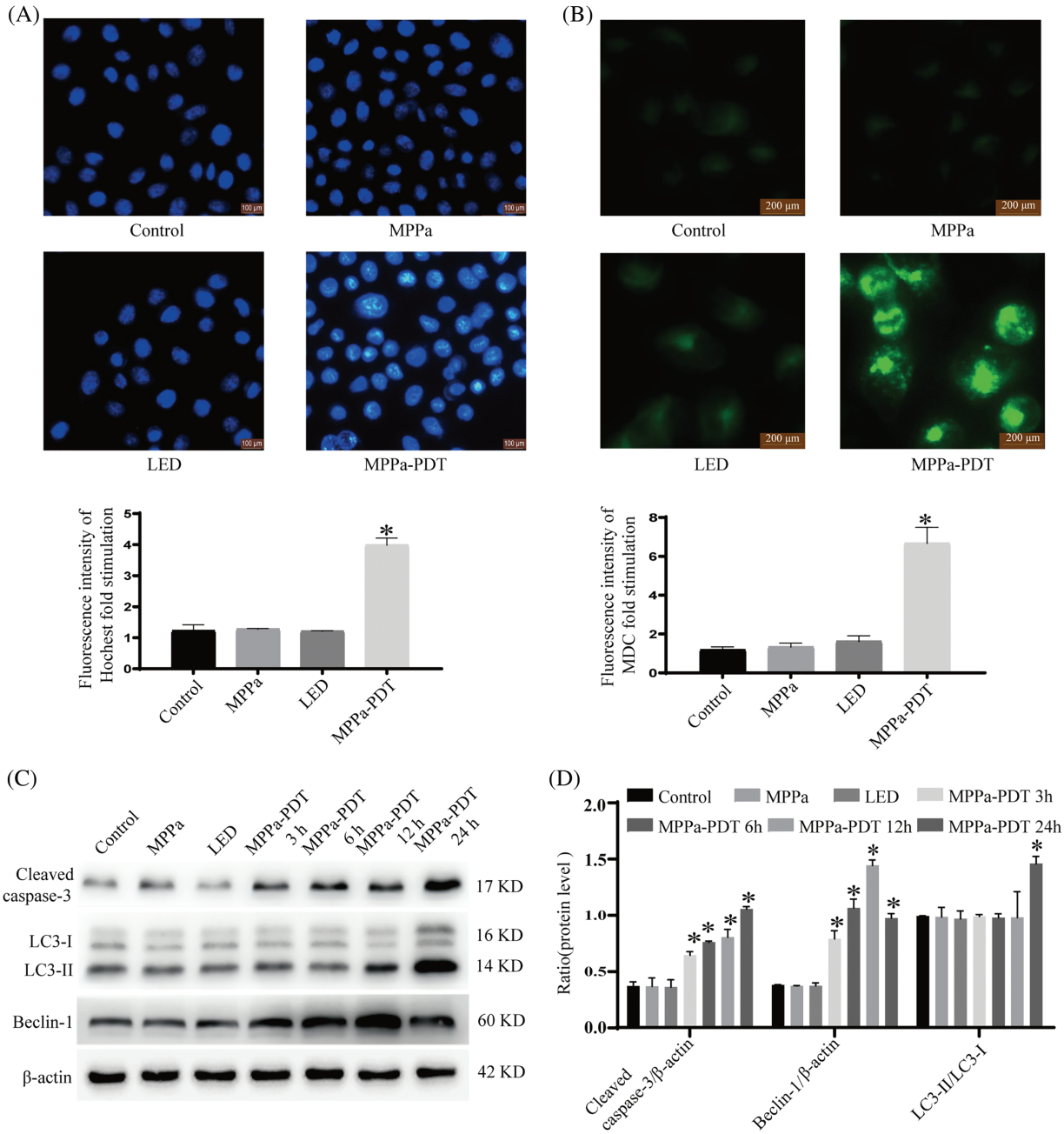

FIGURE 3. MPPa-PDT caused A549 cell apoptosis and autophagy phenomenon. (A) Apoptotic bodies were verified by Hoechst 33342. (B) Autophagic vacuoles were observed by MDC staining. (C, D) Apoptosis and autophagy-related proteins were detected after MPPa-PDT treatment. *$p < 0.05$. The procedure was repeated in triplicate.

JNK and p38 MAPK pathways participated in apoptosis and autophagy following MPPa-PDT management

The MAPK is a conserved enzyme that regulates a variety of cellular physiological events, such as proliferation, differentiation, migration, and survival processes [23]. The results of our study indicated that the MPPa-PDT group exhibited a higher expression level of phosphorylated JNK and phosphorylated p38 than the control group. Still, there was a decrease in phosphorylated ERK expression (Fig. 6A,B). Furthermore, the JNK repressor SP600125 and the particular p38 MAPK suppressant SB203580 dramatically suppressed autophagy and apoptosis (Fig. 6C–F). With the addition of inhibitor U0126, the level of p-ERK further decreased, and evidently, attenuated MPPa-PDT-induced LC3-II protein accumulations accompanying apoptosis increased (Fig. 6G,H). This research demonstrated that A549 cell's autophagy and apoptosis were brought on by MPPa-PDT treatment through JNK and p38 pathways.

Discussion

Photodynamic therapy is a promising approach employed to treat a variety of malignancies [24,25]. In contrast to conventional surgery and chemotherapy, it further eliminates residual tumor cells and drug tolerance by activating the body's anti-cancer immune defenses. MPPa-PDT has been studied deeply in several cancers [26,27].

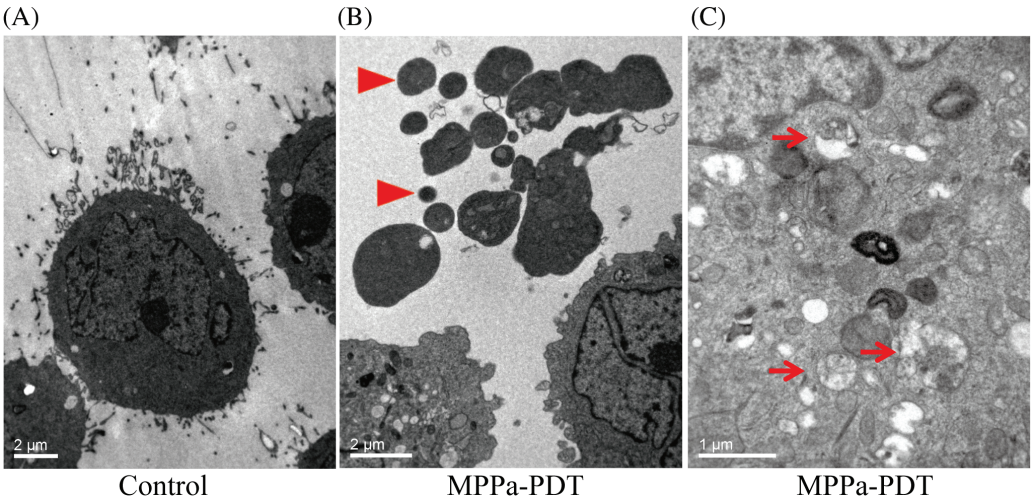

FIGURE 4. Cell ultrastructure was observed under transmission electron micrograph. (A) Normal-appearing A549 cells showed intact cell membranes and nucleus. (B) Cell pseudopodia structure disappeared and apoptotic body formed after MPPa-PDT processing (arrowhead, magnification, ×6000). (C) Autophagosome containing degraded cellular debris was observed after MPPa-PDT treatment (arrow, magnification, ×12,000).

Chen et al. [28] claimed that MPPa-PDT exhibited anti-tumor effects on human osteosarcoma by inhibiting cell proliferation, migration, and invasion. The matrix metalloproteinase-9 (MMP-9) pathway was demonstrated in a recent experiment to be the mechanism by which MPPa-PDT killed breast cancer cells [29]. Our earlier study found that MPPa-PDT caused lung cancer apoptosis via the Caspase-3 pathway [15]. Furthermore, this research showed

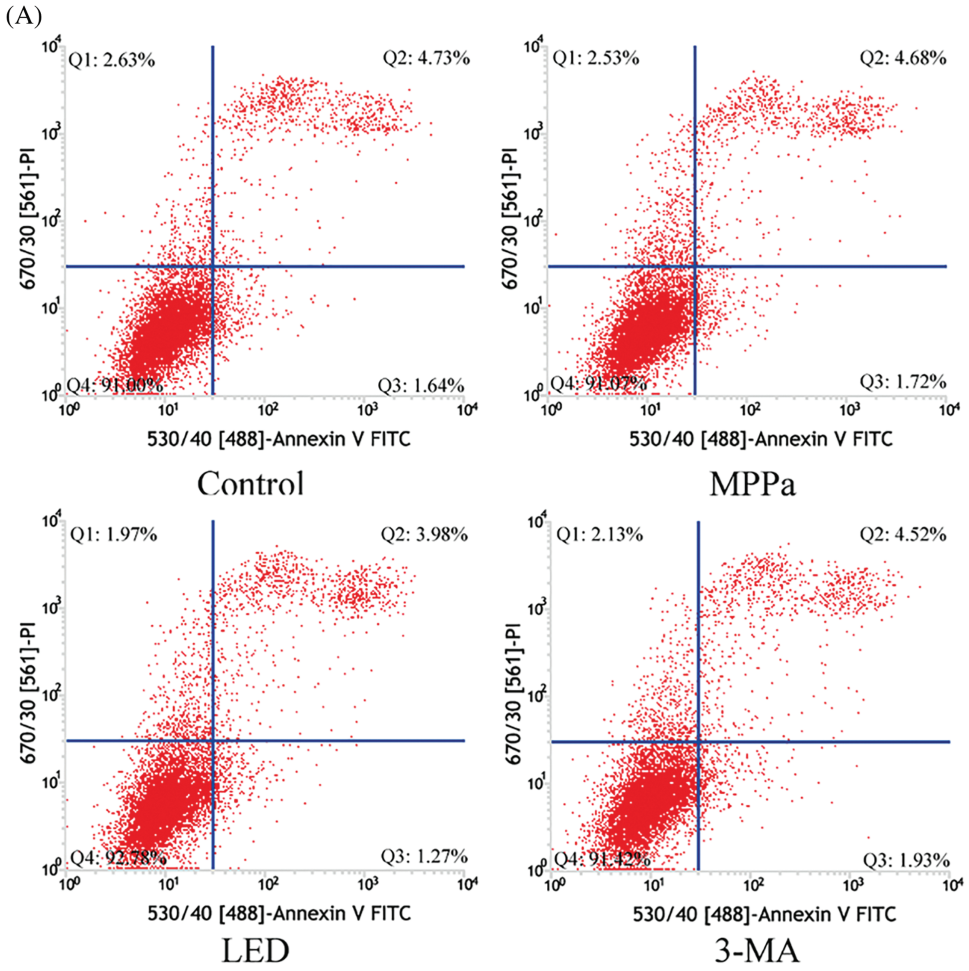

FIGURE 5. (Continued)

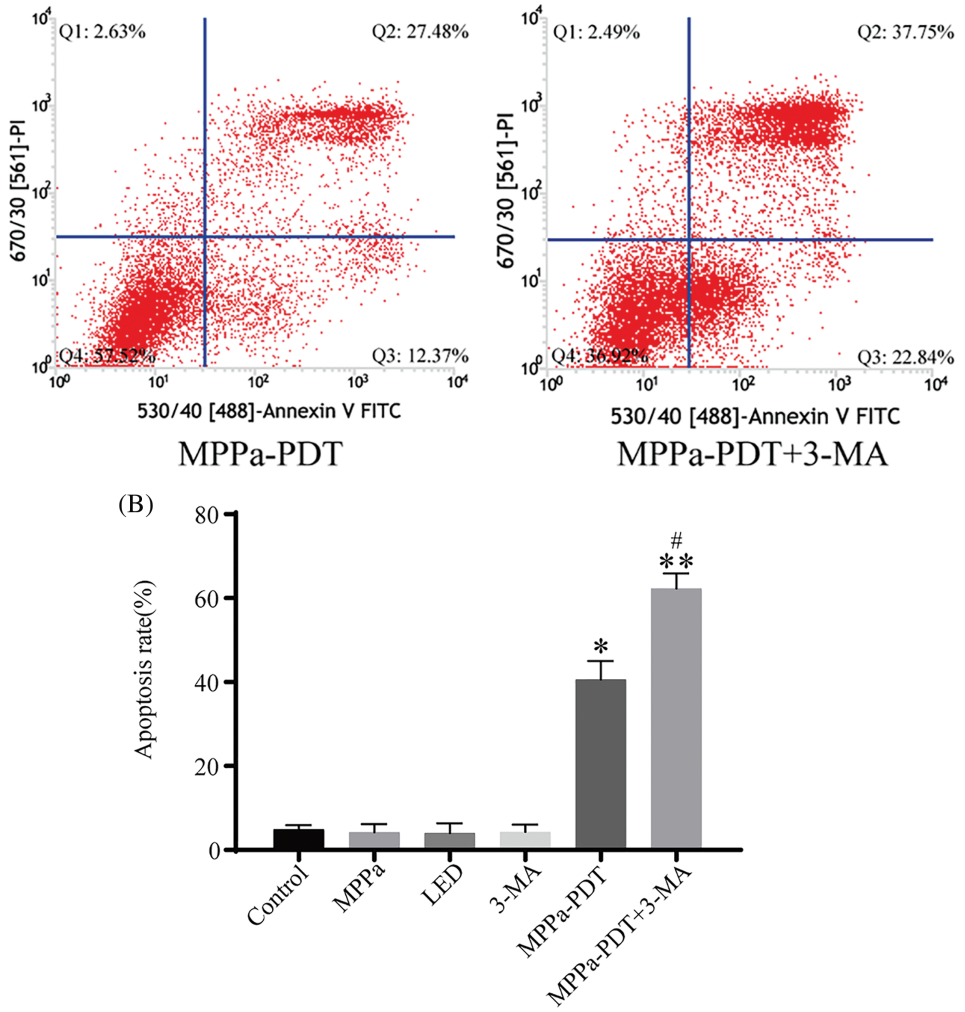

FIGURE 5. Correlations between autophagy and apoptosis due to MPPa-PDT. (A, B) The apoptosis rate was assessed using flow cytometry following the corresponding treatment. Comparatively to the control group, $^{*}p < 0.05$; similarly, in the MPPa-PDT+3-MA group, $^{**}p < 0.01$; $^{\#}p < 0.05$ *vs.* the MPPa-PDT group.

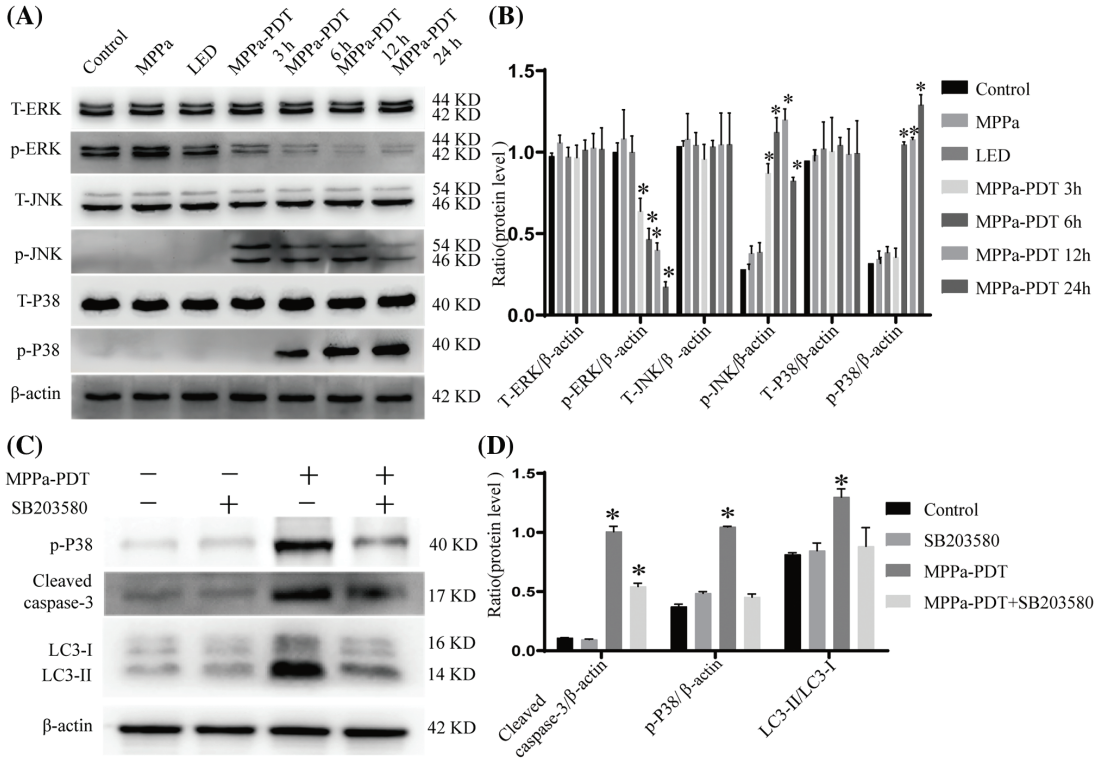

FIGURE 6. (Continued)

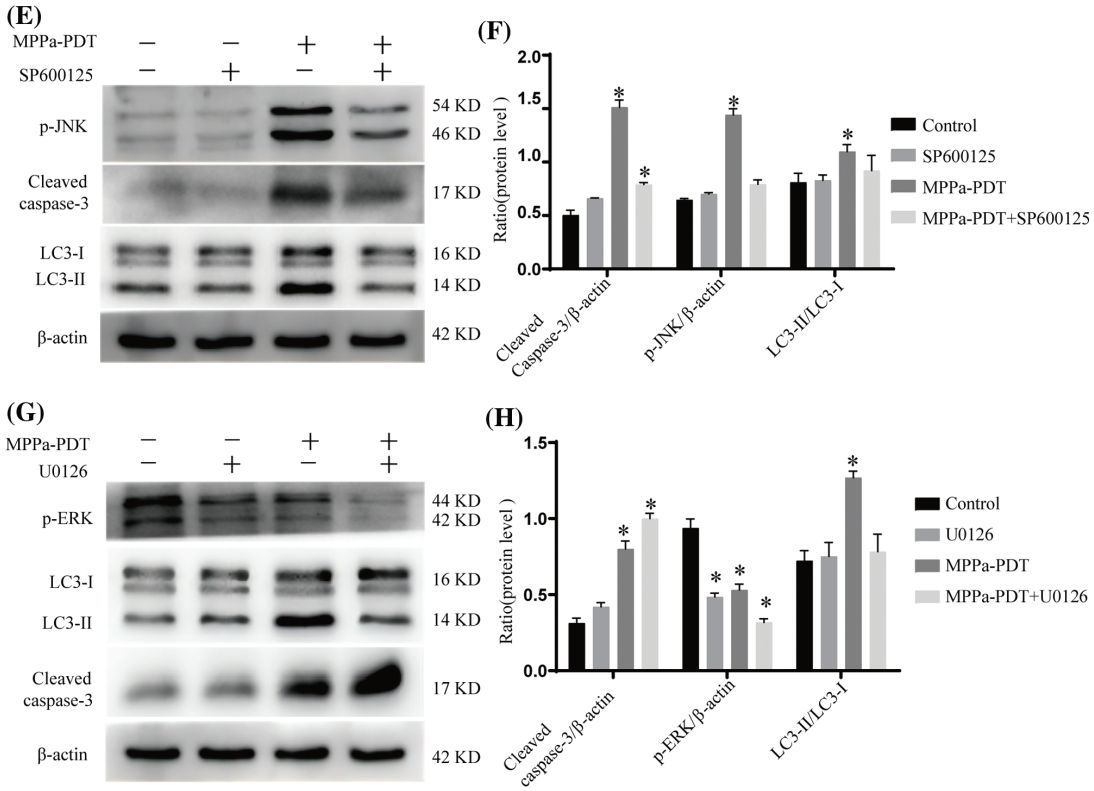

FIGURE 6. MAPK participated in apoptosis and autophagy activated by MPPa-PDT. (A, B) MPPa-PDT activated JNK and p38 MAPK signaling pathway in A549 cells. (C, D) Western blotting for the protein levels of p-38 MAPK, cleaved Caspase-3, and LC3-II/I. The cells were pretreated with SB203580 (p38 inhibitor, 10 μM) for 1 h then followed by processing with or without MPPa-PDT for 24 h. (E, F) For 1 h before being treated with or without MPPa-PDT for 24 h, SP600125 (JNK inhibitor, 20 μM) was preadded to A549 cells. Then detected p-JNK, cleaved Caspase-3, and LC3-II/I expression. (G, H) A549 cells were prepared with U0126 (ERK inhibitor, 20 μM), for 1 h then followed by processing with or without MPPa-PDT for 24 h. Triplicate analyses were conducted. $^*p < 0.05$.

that processing A549 cells with MPPa-PDT triggered apoptosis and autophagy. Based on current research, we first report the link between autophagy and apoptosis produced by MPPa-PDT in the A549 cell line.

The key processes causing cell death are apoptosis and autophagy. Classical cellular staining, transmission electron microscopy, and the expression of specific marker proteins were employed in this study to corroborate apoptosis and autophagy events. Hoechst 33342 staining and transmission electron microscopy revealed that typical apoptotic shape, whereas a western blot in A549 cells with MPPa-PDT management showed the traditional apoptotic hallmark Caspase-3. In addition, Annexin V/PI labeling was used to quantify the apoptosis rate using flow cytometry. Also, MDC staining and transmission electron microscopy confirmed that MPPa-PDT therapy resulted in the production of massive autophagic vacuoles in A549 cells. Furthermore, the MPPa-PDT-treated cells could express higher Beclin1 and LC3-II levels, two indicators of autophagy.

The relationship between apoptosis and autophagy is a hot research topic, but its detailed mechanisms have not been fully clarified. Abundant, reliable evidence validated that autophagy inhibition enhanced cancer therapeutic efficacy [30,31]. MPPa-PDT treatment might trigger an interaction between apoptosis and autophagy. Therefore, we further explored whether MPPa-PDT-induced apoptosis could be affected by the inhibition of autophagy. With the addition of 3-MA, an autophagy inhibitor, the apoptotic rate of A549 cells increased against the MPPa-PDT group. Our findings indicated that autophagy might protect cells by inhibiting apoptosis, while suppressing autophagy may enhance anti-tumor activity.

Accumulating evidence revealed that MAPK signaling pathways were involved in apoptosis and autophagy regulation [32,33]. Researchers have demonstrated that upregulation of p-JNK and p-p38MAPK induced cell apoptosis, whereas p-ERK activation caused cell survival [34,35]. MPPa-PDT treatment activated p-JNK and p-p38 MAPK and caused apoptosis and autophagy by activating both pathways. A549 cells were pretreated with SP600125 (a JNK suppressant) or SB203580 (a p38 MAPK repressor) to confirm whether both signaling regulated apoptosis and autophagy. The treatment of SP600125 or SB203580 decreased JNK and p38 MAPK phosphoryla- tion levels and significantly altered apoptotic and autophagic protein expression. Co-treatment of SP600125 or SB203580 with MPPa-PDT down-regulated Caspase-3 and LC3-II production compared to MPPa-PDT intervention. However, the apoptotic marker was upregulated and the autophagy level was downregulated after p-ERK inhibitor U0126 treatment. Therefore, MPPa-PDT induced apoptosis and autophagy through JNK and p38 MAPK approach in A549 cells.

In conclusion, we claimed that MPPa-PDT caused JNK and p38 MAPK signaling upregulation then further

activated apoptosis and autophagy in A549 cells. In addition, autophagy played a cytoprotective role in lung carcinoma cells treated by MPPa-PDT. However, the limitations of this study should be mentioned. This study was primarily based on A549 cell lines, multiple lung cancer cell lines even animal model experiments that needed further investigation. Additionally, further investigation was necessary to enhance the antineoplastic activity of MPPa-PDT treatment by regulating autophagy and apoptosis.

Acknowledgement: None.

Funding Statement: The study was supported by Xiaogan City Natural Science Foundation of China (Grant/Award No. XGKJ2022010004).

Author Contributions: The authors confirm contribution to the paper as follows: Study conception and design: Zhanling Wu, Kelan Deng; data collection: Xinjun Li; analysis and interpretation of results: Shanshan Wang; draft manuscript preparation: Pinghua Tu, Zhanling Wu. All authors reviewed the results and approved the final version of the manuscript.

Availability of Data and Materials: The datasets generated during and/or analyzed during the current study are available from the corresponding author on reasonable request.

Ethics Approval: Not applicable.

Conflicts of Interest: The authors declare that they have no conflicts of interest to report regarding the present study.

References

1. Mederos N, Friedlaender A, Peters S, Addeo A. Gender-specific aspects of epidemiology, molecular genetics and outcome: lung cancer. ESMO Open. 2020;5(Suppl 4):e000796. doi:10.1136/esmoopen-2020-000796.
2. Wang M, Su X, Hu Y, Yang J. Trends in cancer mortality among the elderly in China, 2005–2035. PLoS One. 2024;19(5):e0302903. doi:10.1371/journal.pone.0302903.
3. Alexander M, Kim SY, Cheng H. Update 2020: management of non-small cell lung cancer. Lung. 2020;198(6):897–907. doi:10.1007/s00408-020-00407-5.
4. Xiu J, Wang S, Wang X, Xu W, Hu Y, Hua Y, et al. Effectiveness and safety of segmentectomy *vs.* wedge resection for the treatment of patients with operable non-small cell lung cancer: a meta-analysis and systematic review. Oncol Lett. 2024;28(1):336. doi:10.3892/ol.2024.14469.
5. Yao D, Zhu X, Guo J, Dong X, Zeng Y, Fu X, et al. A real-world analysis of stereotactic body radiotherapy combined with immunotherapy in advanced or recurrent non-small cell lung cancer (NSCLC): a single-center experience. Clin Transl Radiat Oncol. 2024;47:100787. doi:10.1016/j.ctro.2024.100787.
6. Mei Y, Gu L, Chen Y, Zhang P, Cheng Y, Yuan R, et al. A novel photosensitizer based 450-nm blue laser-mediated photodynamic therapy induces apoptosis in colorectal cancer-*in vitro* and *in vivo* study. Front Biosci (Landmark Ed). 2024;29(5):199. doi:10.31083/j.fbl2905199.
7. Mokoena D, George BP, Abrahamse H. Cannabidiol combination enhances photodynamic therapy effects on MCF-7 breast cancer cells. Cells. 2024;13(2):187. doi:10.3390/cells13020187.
8. Li X, Lovell JF, Yoon J, Chen X. Clinical development and potential of photothermal and photodynamic therapies for cancer. Nat Rev Clin Oncol. 2020;17(11):657–74. doi:10.1038/s41571-020-0410-2.
9. Guo T, Lin W, Chen W, Huang Y, Zhu L, Pan X. Photodynamic therapy in combination with sorafenib for enhanced immunotherapy of lung cancer. J Biomed Nanotechnol. 2020;16(8):1219–28. doi:10.1166/jbn.2020.2970.
10. Alvim RG, Georgala P, Nogueira L, Somma AJ, Nagar K, Thomas J, et al. Combined OX40 agonist and PD-1 inhibitor immunotherapy improves the efficacy of vascular targeted photodynamic therapy in a urothelial tumor model. Molecules. 2021;26(12):3744. doi:10.3390/molecules26123744.
11. Liang L, Bi W, Chen W, Lin Y, Tian Y. Combination of MPPa-PDT and HSV1-TK/GCV gene therapy on prostate cancer. Lasers Med Sci. 2018;33(2):227–32. doi:10.1007/s10103-017-2331-6.
12. Huang Q, Ou YS, Tao Y, Yin H, Tu PH. Apoptosis and autophagy induced by pyropheophorbide-α methyl ester mediated photodynamic therapy in human osteosarcoma MG-63 cells. Apoptosis. 2016;21(6):749–60. doi:10.1007/s10495-016-1243-4.
13. Qian G, Wang L, Zheng X, Yu T. Deactivation of cisplatin-resistant human lung/ovary cancer cells with pyropheophorbide—a methyl ester-photodynamic therapy. Cancer Biol Ther. 2017;18(12):984–9. doi:10.1080/15384047.2017.1385683.
14. Zhu J, Tian S, Li KT, Chen Q, Jiang Y, Lin HD, et al. Inhibition of breast cancer cell growth by methyl pyropheophenylchlorin photodynamic therapy is mediated though endoplasmic reticulum stress-induced autophagy *in vitro* and *vivo*. Cancer Med. 2018;7(5):1908–20. doi:10.1002/cam4.1418.
15. Tu PH, Huang WJ, Wu ZL, Peng QZ, Xie ZB, Bao J, et al. Induction of cell death by pyropheophorbide-α methyl ester-mediated photodynamic therapy in lung cancer A549 cells. Cancer Med. 2017;6(3):631–9. doi:10.1002/cam4.1012.
16. Silva VR, Neves SP, Santos LS, Dias RB, Bezerra DP. Challenges and therapeutic opportunities of autophagy in cancer therapy. Cancers. 2020;12(11):3461. doi:10.3390/cancers12113461.
17. Xiao M, Benoit A, Hasmim M, Duhem C, Vogin G, Berchem G, et al. Targeting cytoprotective autophagy to enhance anticancer therapies. Front Oncol. 2021;25(11):626309. doi:10.3389/fonc.2021.626309.
18. Wang FT, Wang H, Wang QW, Pan MS, Li XP, Sun W, et al. Inhibition of autophagy by chloroquine enhances the antitumor activity of gemcitabine for gallbladder cancer. Cancer Chemother Pharmacol. 2020;86(2):221–32. doi:10.1007/s00280-020-04100-5.
19. Huang G, He X, Xue Z, Long Y, Liu J, Cai J, et al. Rauwolfia vomitoria extract suppresses benign prostatic hyperplasia by inducing autophagic apoptosis through endoplasmic reticulum stress. BMC Complement Med Ther. 2022;22(1):125. doi:10.1186/s12906-022-03610-4.
20. Zhang X, Gao H, Wei D, Pei X, Zhang Y, Wang J, et al. ROS responsive nanoparticles encapsulated with natural medicine remodel autophagy homeostasis in breast cancer. ACS Appl Mater Interfaces. 2023;15(25):29827–29840. doi:10.1021/acsami.3c03068.

21. Li X, Gu L, Chen Y, Wang X, Mei Y, Zhou J, et al. A novel 450-nm laser-mediated sinoporphyrin sodium-based photodynamic therapy induces autophagic cell death in gastric cancer through regulation of the ROS/PI3K/Akt/mTOR signaling pathway. BMC Med. 2022;20(1):475. doi:10.1186/s12916-022-02676-8.
22. Tu P, Huang Q, Ou Y, Du X, Li K, Tao Y, et al. Aloe-emodin-mediated photodynamic therapy induces autophagy and apoptosis in human osteosarcoma cell line MG-63 through the ROS/JNK signaling pathway. Oncol Rep. 2016;35(6):3209–15. doi:10.3892/or.2016.4703.
23. Gagliardi PA, Pertz O. The mitogen-activated protein kinase network, wired to dynamically function at multiple scales. Curr Opin Cell Biol. 2024;88:102368. doi:10.1016/j.ceb.2024.102368.
24. Casas A. Clinical uses of 5-aminolaevulinic acid in photodynamic treatment and photodetection of cancer: a review. Cancer Lett. 2020;10(490):165–73. doi:10.1016/j.canlet.2020.06.008.
25. Usuda J, Inoue T, Tsuchida T, Ohtani K, Maehara S, Ikeda N, et al. Clinical trial of photodynamic therapy for peripheral-type lung cancers using a new laser device in a pilot study. Photodiagnosis Photodyn Ther. 2020;30:101698. doi:10.1016/j.pdpdt.2020.101698.
26. Sun X, Leung WN. Photodynamic therapy with pyropheophorbide-α methyl ester in human lung carcinoma cancer cell: efficacy, localization and apoptosis. Photochem Photobiol. 2002;75(6):644–51. doi:10.1562/0031-8655(2002)075<0644:PTWPAM>2.0.CO;2.
27. Pan L, Lin H, Tian S, Bai D, Kong Y, Yu L. The sensitivity of glioma cells to pyropheophorbide-α methyl ester-mediated photodynamic therapy is enhanced by inhibiting ABCG2. Lasers Surg Med. 2017;49(7):719–26. doi:10.1002/lsm.22661.
28. Chen Y, Yin H, Tao Y, Zhong S, Yu H, Li J, et al. Antitumor effects and mechanisms of pyropheophorbide-α methyl ester-mediated photodynamic therapy on the human osteosarcoma cell line MG-63. Int J Mol Med. 2020;45(4):971–82. doi:10.3892/ijmm.2020.4494.
29. Huang L, Lin H, Chen Q, Yu L, Bai D. MPPa-PDT suppresses breast tumor migration/invasion by inhibiting Akt-NF-κB-dependent MMP-9 expression via ROS. BMC Cancer. 2019;19(1):1159. doi:10.1186/s12885-019-6374-x.
30. Nakatani K, Matsuo H, Harata Y, Higashitani M, Koyama A, Noura M, et al. Inhibition of CDK4/6 and autophagy synergistically induces apoptosis in t(8;21) acute myeloid leukemia cells. Int J Hematol. 2021;113(2):243–53. doi:10.1007/s12185-020-03015-4.
31. Hao M, Zhang C, Shi N, Yuan L, Zhang T, Wang X. Procaine induces cell cycle arrest, apoptosis and autophagy through the inhibition of the PI3K/AKT and ERK pathways in human tongue squamous cell carcinoma. Oncol Lett. 2024;28(3):408. doi:10.3892/ol.2024.14541.
32. Xu Y, Sun Q, Yuan F, Dong H, Zhang H, Geng R, et al. RND2 attenuates apoptosis and autophagy in glioblastoma cells by targeting the p38 MAPK signalling pathway. J Exp Clin Cancer Res. 2020;39(1):174. doi:10.1186/s13046-020-01671-2.
33. Fan J, Ren D, Wang J, Liu X, Zhang H, Wu M, et al. Bruceine D induces lung cancer cell apoptosis and autophagy via the ROS/MAPK signaling pathway *in vitro* and *in vivo*. Cell Death Dis. 2020;11(2):126. doi:10.1038/s41419-020-2317-3.
34. Innajak S, Mahabusrakum W, Watanapokasin R. Goniothalamin induces apoptosis associated with autophagy activation through MAPK signaling in SK-BR-3 cells. Oncol Rep. 2016;35(5):2851–8. doi:10.3892/or.2016.4655.
35. Song C, Xu W, Wu H, Wang X, Gong Q, Liu C, et al. Photodynamic therapy induces autophagy-mediated cell death in human colorectal cancer cells via activation of the ROS/JNK signaling pathway. Cell Death Dis. 2020;11(10):938. doi:10.1038/s41419-020-03136-y.